

# Free Rotation of Magnetic Nanoparticles in a Solid Matrix

E. del Barco, J. Asenjo, X. X. Zhang, R. Pieczynski, A. Julià, J. Tejada,\* and R. F. Ziolo\*

University of Barcelona Xerox Laboratory, Avda. Diagonal 647, 08028 Barcelona, Spain

D. Fiorani and A. M. Testa

ICMAT CNR, Area della Ricerca di Roma, Rome, Italy

Received July 4, 2000. Revised Manuscript Received January 17, 2001

Magnetic data for a composite material consisting of nanocrystalline  $\gamma$ -Fe<sub>2</sub>O<sub>3</sub> dispersed in an alginate methanol matrix indicate the presence of rotationally free magnetic particles. The decoupling of the particles from the matrix was achieved by subjecting the sample to a magnetic field applied in alternating directions. Before field treatment, a magnetic blocking process is observed at low temperature, which is characteristic of nanoscale magnetic materials in the presence of barriers for the magnetic moment of the particles. After the field treatment, no magnetic hysteresis is observed and the magnetization follows a Curie–Weiss law. This behavior can only be interpreted as due to magnetic moments that follow the external magnetic field without delay, implying, therefore, the existence of free particles.

## 1. Introduction

The existence of a rotationally free magnet, such as a compass needle, can be easily verified experimentally because of its preferred orientation in an applied magnetic field. In contrast, a magnetic crystal or particle that is not free to rotate has an energy minimum determined by its anisotropy energy. In magnetic composites consisting of nanoscale magnetic particles dispersed in a solid matrix, the particulate is usually firmly embedded in the matrix and bonded to it. Both factors contribute to the prevention of any local movement of the particulate. Typically, such materials show magnetic hysteresis below a blocking temperature,  $T_B$ , and superparamagnetism above  $T_B$ .

Recently, the first example of a nanocomposite containing rotationally free nanomagnets was demonstrated in a material consisting of nanocrystalline  $\gamma$ -Fe<sub>2</sub>O<sub>3</sub> dispersed in a functionalized polystyrene methanol matrix.<sup>1</sup> The magnetic data indicated that the particles undergo free rotation in response to an applied magnetic field after cyclic field treatment of the solid matrix. These data also suggested that the effect might occur in a matrix that was structurally weak, at least in the vicinity of the iron oxide particle and, alternatively, in one that might possess weak particle matrix interactions and cavities.<sup>1</sup> In such cases, the application of a sufficiently strong cyclic magnetic field could break the particle–matrix coupling.

To demonstrate the free rotor phenomenon in a second and independent matrix, we have characterized the magnetic properties of a nanocomposite prepared

from a methanol ferrofluid of  $\gamma$ -Fe<sub>2</sub>O<sub>3</sub> and a naturally occurring polysaccharide, commonly known as alginate.<sup>2</sup> The data are compared with those obtained from a second series of measurements on the sample used in our original work.<sup>1</sup>

## 2. Experimental Section

Both samples were prepared as reported previously.<sup>1,2</sup> Sample 1 consisted of a methanol ferrofluid containing nanocrystalline  $\gamma$ -Fe<sub>2</sub>O<sub>3</sub> and alginate, a naturally occurring polysaccharide. Sample 2 was the original methanol ferrofluid sample from our earlier work<sup>1</sup> and contained nanocrystalline  $\gamma$ -Fe<sub>2</sub>O<sub>3</sub> and sulfonated polystyrene. The second series of measurements performed on the original polystyrene sample and reported on here were done several months after the initial measurements. Multiple loadings of the resins resulted in 51% and 57% iron oxide for the dried polysaccharide and polystyrene resins, respectively. Both samples solidify at  $\approx 200$  K. Transmission electron microscopy measurements that showed 5–10-nm equi-axed or spherical particles have been illustrated previously.<sup>3</sup> The average particle diameter for the two samples deduced from the low-field magnetic measurements was 7.4 nm for sample 1 and 12.1 nm for sample 2. Phase purity of the samples was determined using selected area electron diffraction analysis and optical spectrophotometry.<sup>3–5</sup> Magnetic measurements were performed on a commercial SQUID magnetometer.

## 3. Results and Discussion

Magnetization vs temperature measurements for both zero-field-cooled (ZFC) and field-cooled (FC) processes

(2) Kroll, E.; Winnik, F. M.; Ziolo, R. F. *Chem. Mater.* **1996**, *8*, 1594.

(3) Ziolo, R. F.; Giannelis, E. P.; Weinstein, B. A.; O'Horo, M.; Ganguly, B. N.; Mehrotra, V.; Russell, M. W.; Huffman, D. R. *Science* **1992**, *257*, 219.

(4) Vassiliou, J. K.; Mehrotra, V.; Russell, M. W.; Giannelis, E. P.; McMichael, R. D.; Shull, R. D.; Ziolo, R. F. *J. Appl. Phys.* **1993**, *73*, 5109–5116.

(5) Klapczynski, T.; Galeski, A.; Kryszewski, M. *J. Appl. Polym. Sci.* **1995**, *58*, 1007.

\* To whom correspondence should be addressed. Tel.: (34)93 4021158. Fax: (34)93 4021149. E-mail: jtejada@ubxlab.com, rziolo@ubxlab.com.

(1) Tejada, J.; Zhang, X. X.; Kroll, E. C.; Bohigas, X.; Ziolo, R. *J. Appl. Phys.* **2000**, *87*, 8008–8012.

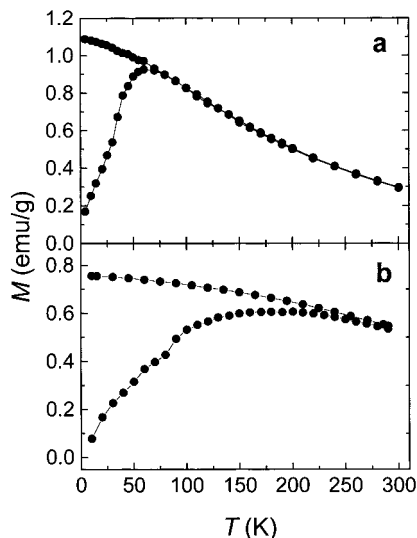


**Figure 1.** Zero-field-cooled (ZFC) and field-cooled (FC) magnetization curves at  $H = 200$  Oe for sample 1 (a) and at  $H = 100$  Oe for sample 2 (b).

are reported in Figure 1a,b for samples 1 and 2, respectively. Both samples behave as expected for an ensemble of magnetic nanoparticles with a volume distribution  $f(V)$ .<sup>6</sup> That is, there is a distribution for both energy barriers,  $U (U = KV)$ , and relaxation times,  $\tau = \tau_0 \exp(U/K_B T)$ , which give rise to different magnetization values, depending on if the sample is cooled in the absence or the presence of a magnetic field. When a sample is cooled in zero field, the total magnetization will be zero since the magnetic moments of the particles are randomly oriented. The application of a magnetic field, however, induces a net magnetic moment along the field direction, which will increase with temperature as more and more particles orient their magnetic moments parallel to the field. This is the ZFC curve, which at each temperature, represents the magnetization of those particles having a certain volume,  $V$ , for which their relaxation time equals the experimental window time. At the temperature at which the relaxation time of most of the magnetic moments of particles equal the experimental resolution time, the ZFC curve comes to a maximum, which corresponds to the case when the majority of the particles behave superparamagnetically. This temperature is the blocking temperature,  $T_B$ . At temperatures higher than  $T_B$ , the magnetization decreases as seen for sample 1 and follows a Curie–Weiss law corresponding to the superparamagnetic behavior. This is the regime where the thermal energy is greater than the anisotropy barrier heights. The Curie–Weiss temperature for sample 1, deduced from the magnetization data above  $T_B$ , is about 50 K. For sample 2, clear Curie–Weiss behavior is not observed above  $T_B$  and may be indicative of the existence of dipole–dipole interaction between the particles. Such behavior has been reported for several particle systems,<sup>7–10</sup>

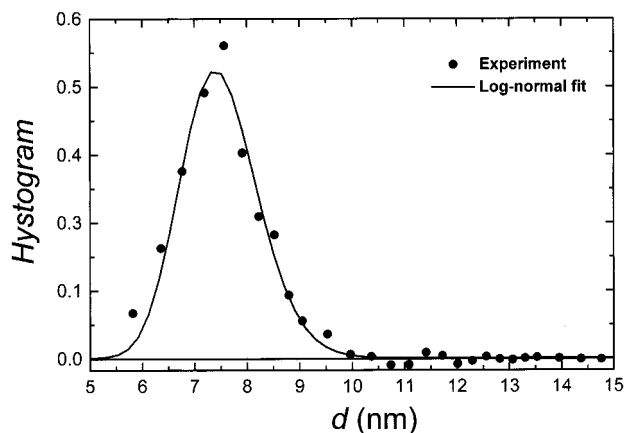


**Figure 2.** Volume distribution for the particles of sample 1 deduced from the low field magnetic measurements (ZFC–FC curves).

in agreement with theoretical prediction<sup>11</sup> and the results of Monte Carlo simulations.<sup>12,13</sup>

If a sample is cooled from the superparamagnetic state in the presence of a magnetic field to generate the FC curve, both the FC (equilibrium magnetization) and ZFC curves coincide until  $T_B$ . Below  $T_B$ , the FC curve splits from the ZFC curve since it does not correspond to the equilibrium. Moreover, the ZFC curve relaxes toward the FC curve. That is, below  $T_B$ , blocking of the magnetic moments occurs for times longer than the experimental resolution time. There are metastable states separated by energy barriers, which prevent a free magnetization reversal, and both relaxation and hysteresis phenomena are observed. The ZFC curve is fully determined, therefore, by the barrier height distribution. Consequently, the volume distribution of the particle ensemble may be deduced from the ZFC curve. The accuracy of this method is influenced by the presence of interaction between particles. That is, in the strictest sense we are determining the barrier height distribution resulting from both the anisotropy height and the dipole–dipole interaction between particles. In Figure 2, we show the volume distribution for sample 1 deduced from the ZFC and FC curves shown in Figure 1a.

The blocking temperature of sample 2 is about 100 K higher than that for sample 1, where  $T_B = 60$  K. The difference is related to the different average sizes of the samples, which is larger for sample 2 (about 12 nm vs 7.4 for sample 1) and to the existence of a broader distribution of energy barriers. The latter is indicated by the much broader maximum in the ZFC curve of sample 2. The 12-nm average size deduced for sample 2 from the ZFC–FC curves is higher than the value suggested by the data of transmission microscopy (5–10 nm). We believe that this discrepancy may be due to the fact that in sample 2 the dipole–dipole

(6) Dormann, J. L.; Fiorani, D.; Tronc, E. *Adv. Chem. Phys.* **98**, 283, 1997.

(7) Coffey, W. T.; Crothers, D. S. F.; Dormann, J. L.; Geoghegan, L. J.; Kennedy, E. C. *Phys. Rev. B* **1998**, *58*, 3249; Coffey, W. T.; Crothers, D. S. F.; Kalmykov, Yu. P.; Waldron, J. T. *Phys. Rev. B* **1995**, *51*, 15947.

(8) Dormann, J. L.; D’Orazio, F.; Lucari, F.; Tronc, E.; Pren, P.; Jolivet, J. P.; Fiorani, D.; Cherkaoui, R.; Nogues, M. *Phys. Rev. B* **1996**, *53*, 14291.

(9) Jonsson, T.; Nordblad, P.; Svedlindh, P. *Phys. Rev. B* **1998**, *57*, 497.

(10) Mamiya, H.; Nakatani, I.; Furubayashi, T. *Phys. Rev. Lett.* **1998**, *80*, 177.

(11) Dormann, J. L.; Bessais, L.; Fiorani, D. *J. Phys. C* **1988**, *21*, 2015.

(12) Chantrell, R. W.; Walmsley, N. S.; Gore, J.; Maylin, M. *J. Magn. Magn. Mater.* **1999**, *196–197*, 118.

(13) Garcia-Otero, J.; Porto, M.; Rivas, J.; Bunde, A. *Phys. Rev. Lett.* **2000**, *84*, 167.

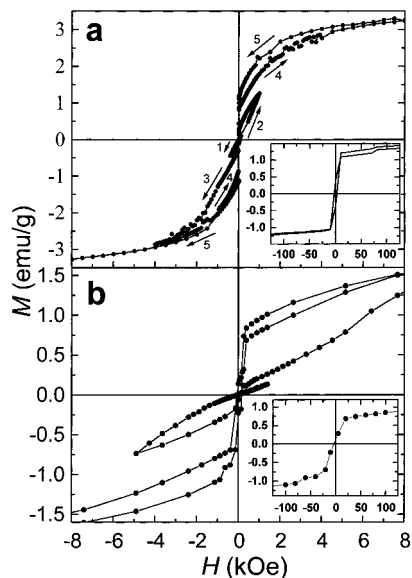


**Figure 3.** Magnetization as a function of the applied field measured at 4.2 K after the field treatment at  $\pm 30$  kOe: (a) sample 1; (b) sample 2. Arrows point the way in which the magnetic field was varied. Insets: low field detail.

interaction between particles is large. That is, in the presence of dipolar interaction between particles the barrier height distribution deduced from the ZFC–FC curves does not fully correspond to the volume distribution.<sup>6</sup> For sample 2, the FC magnetization curve increases very slowly with decreasing temperature and tends to flatten off. Its temperature behavior is definitively different from the  $1/T$  Curie-like law expected for noninteracting particles and suggests the presence of non-negligible interparticle interactions, presumably of the dipole–dipole type.

A significant change in the magnetic properties of both nanocomposites occurs when the magnetic field is cycled below  $T_{\max}$ . Figure 3 shows the  $M(H)$  curves at 4.2 K for both samples, measured after zero field cooling and a subsequent field treatment. For sample 1, the field treatment consisted of a sequence of minor loops performed as follows: the field was increased to a positive value,  $H_1 = 100$  Oe, and then decreased to a negative value,  $H_2 = -400$  Oe, larger than the previous positive value. This procedure was repeated by increasing the amplitude of the applied field up to 15 kOe, the last applied field. Unlike hard magnetic materials, where  $H_c$  increases with the strength of the applied field up to a constant value, there is no evidence for a finite coercive field for any applied field up to its maximum value. Moreover, the magnetization reversal occurs at near zero applied field. Likewise, the same behavior was observed for sample 2 using the field treatment of  $+30$  to  $-30$  kOe reported earlier.<sup>1</sup>

After field treatment, the magnetization of both samples was measured as a function of increasing temperature in an applied field of 20 Oe starting from 4.2 K after a ZFC process from 250 K. The resulting curves differ from the ZFC curves measured before the field treatment and are shown in Figure 4. Here, the magnetization decreases with temperature and no maxima are observed as in the case before the field treatment (Figure 1). The data indicate that the particles behave as though they were in the superpara-

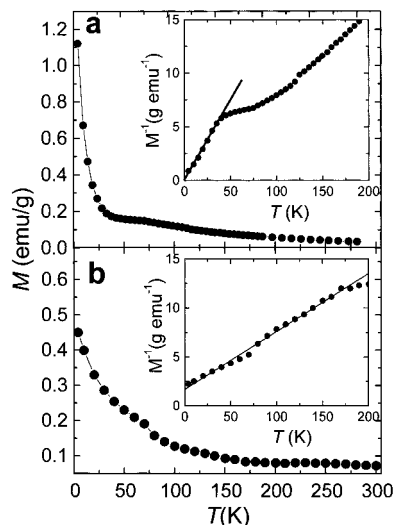


**Figure 4.** Zero-field-cooled magnetization vs temperature measured at  $H = 20$  Oe for sample 1 and  $H = 20$  Oe for sample 2 after the field treatment at  $\pm 30$  kOe: (a) sample 1; (b) sample 2. Insets:  $M^{-1}$  vs temperature.

magnetic state with no observed blocking of the particle moments. The same behavior was reported for the magnetic nanoparticle in the polystyrene methanol matrix and is indicative of an ensemble of freely rotating magnetic particles.<sup>1</sup> In other words, these data suggest that there are no barriers for the magnetic moments, which at low temperature are mostly oriented along the direction of the magnetic field. When the temperature is increased, the alignment of the magnetic moment along the field direction decreases and, consequently, the magnetization decreases when the temperature is increased.

We note that whereas sample 2 exhibits Curie–Weiss behavior in the whole temperature range (inset, Figure 4b), the linear temperature dependence of  $M^{-1}$  for sample 1 is found only below 40 K (inset, Figure 4a). The Curie–Weiss temperature deduced from these magnetization data is close to zero for sample 1 and  $-30$  K for sample 2. This suggests that the dipole–dipole interaction between the particles in the free rotor state is larger in sample 2 than in sample 1. This result is in agreement with that obtained from the initial magnetization data above the blocking temperature. The observed  $M^{-1}$  vs  $T$  curve can be fitted as the sum of a Curie–Weiss term due to free particles and a log-normal term accounting for a distribution of blocking temperatures for the matrix-fixed particles. These results suggest that, for sample 1, only a fraction of particles are free to rotate in contrast to the nearly complete free rotation observed in sample 2. The fraction of free particles for sample 1 deduced from the above-mentioned fitting is 90%. The difference between the two samples may result from the different natures of the matrixes, different preparative histories, and differences between the field treatments and average particle sizes.

Figure 5 shows the magnetization as a function of time for sample 1 before and after the field treatment. Before field treatment, the coercive field at 5 K has a finite value as a result of magnetic anisotropy, and the magnetization decays linearly with the logarithm of time. This behavior is expected for a composite containing nanoscale magnetic particles firmly embedded in

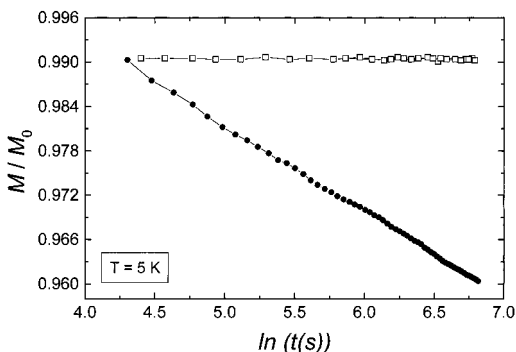


**Figure 5.** Time decay of the remanent magnetization of sample 2 measured at 5 K before (solid circles) and after (open squares) the field treatment at  $\pm 30$  kOe. In both cases, the sample is field-cooled in  $H = 100$  Oe until  $T = 5$  K and then the magnetic field is changed to  $H = -100$  Oe.

and unable to rotate in a matrix. After the field treatment via the “ $\pm$ ” applied field, the magnetization of sample 1 becomes independent of time with  $\Delta M/M$  lower than 0.01%. Thus, after field treatment, magnetic relaxation is no longer observed for the polysaccharide methanol sample at 5 K and  $M(H) = -M(-H)$ , even at small fields.

These results indicate that there are no longer energy barriers to the orientation of the magnetic moments in the direction of the applied magnetic field and that both the magnetic moment and particle itself rotate in the presence of the applied field. The same behavior was observed in the polystyrene methanol matrix<sup>1</sup> and for sample 2. Since some particle interactions are present, it is possible that some interacting particles rotate together in the applied field.

As discussed earlier,<sup>1</sup> the precursors to both methanol-polymer free-rotor systems form thixotropic gels that appear to involve solvent-swollen polymer networks surrounding the magnetic particles. In contrast, at least to date, we have not observed thixotropy in the equivalent water-based systems, nor any free rotor formation upon solidification and field treatment of the water-based systems. Formation of the methanol-polymer free-rotor systems may involve mutually antagonistic surfaces between the particle, which may retain a surfactant layer, and the methanol-polymer matrix, which may be cavernous.<sup>14</sup> Unlike ferrofluid particles, which involve nearly free rotation,<sup>15</sup> particle rotation in the solids case involves no viscous drag. As a consequence, particles can follow small variations in an applied magnetic field without lag or magnetic relaxation.

#### 4. Conclusions

The magnetic characterization of a composite material consisting of nanocrystalline  $\gamma$ - $\text{Fe}_2\text{O}_3$  dispersed in an alginate methanol matrix indicates the presence of rotationally free nanomagnets. As such, the material constitutes the second known free-rotor solid. The free rotation of the particles precludes the observation of magnetic relaxation phenomena that are characteristic of ordinary magnetic solids and ferrofluids.

CM001122T

(14) Hendriksen, P. V.; Moerup, S.; Linderroth, S. *J. Phys. C: Condens. Matt.* **1991**, 3, 3109.

(15) Scholten, P. In *Magnetic Properties of Fine Particles*; Dormann, J. L., Fiorani, D., Eds.; North-Holland: Amsterdam, 1992; p 277.